

Supersolids versus phase separation in two-dimensional lattice bosons

Pinaki Sengupta,¹ Leonid P. Pryadko,¹ Fabien Alet,^{2,3} Matthias Troyer,² and Guido Schmid²

¹Department of Physics, University of California, Riverside, CA 92521

²Theoretische Physik, ETH Zürich, CH-8093 Zürich, Switzerland

³Service de Physique Théorique, CEA Saclay, F-91191 Gif sur Yvette, France

(Dated: November 13, 2018)

We study the nature of the ground state of the strongly-coupled two dimensional extended boson Hubbard model on a square lattice. We demonstrate that strong but finite on-site interaction U along with a comparable nearest-neighbor repulsion V result in a thermodynamically stable supersolid ground state just above half-filling, and that the checker-board crystal is unstable for smaller V , and for any V just below half-filling. The interplay between these two interaction energies results in a rich phase diagram which is studied in detail using quantum Monte Carlo methods.

The detection of possible supersolid (SS) state in recent experiments on solid ⁴He by Kim and Chan [1] has led to renewed interest [2] in a problem that has long [3] intrigued physicists: Can a supersolid phase—with simultaneous diagonal (solid) and off-diagonal (superfluid) long-range order—exist in a bosonic system? While the issue remains controversial [4, 5, 6] in a translationally invariant system despite almost fifty years of theoretical research, the situation in lattice models is clearer.

Theoretical studies [7, 8, 9] of various *lattice* boson models (which can nowadays be implemented using cold bosonic atoms on optical lattices [10]), appeared to confirm that here supersolid ground states can indeed exist, particularly when doped away from half-filling. Studies of the closely related quantum phase model found supersolid order in the ground state even at half-filling [9]. However, as was pointed out recently the stability of the supersolid against phase separation had not been investigated [11]. Indeed, for hard-core bosons on a square lattice, the most widely discussed supersolid pattern—with (π, π) diagonal order—is thermodynamically unstable and phase separates into a pure (π, π) solid and a superfluid (SF) for all values of interaction strengths. A striped supersolid phase—with $(0, \pi)$ ordering—is stabilized by a finite next-nearest-neighbor (nnn) interaction.

In this work we analyze stability of crystalline and supersolid orders of lattice bosons. We present exact strong-coupling arguments showing under which conditions checkerboard supersolids are unstable, and how they can be stabilized with large but finite on-site and nearest-neighbor (nn) energies U and V . We support these arguments by quantum Monte Carlo simulations of a two-dimensional (2D) extended Bose Hubbard model demonstrating that the supersolid (SS) phase is stabilized for densities $\rho > 1/2$ and sufficiently large V (Fig. 1).

Specifically, we study the extended Bose-Hubbard model (EBHM) on a d -dimensional hypercubic lattice with on-site (U) and nn (V) interactions,

$$H = -t \sum_{\langle i,j \rangle} (a_i^\dagger a_j + a_j^\dagger a_i) - \mu \sum_i n_i + V \sum_{\langle i,j \rangle} n_i n_j + \frac{U}{2} \sum_i n_i (n_i - 1), \quad (1)$$

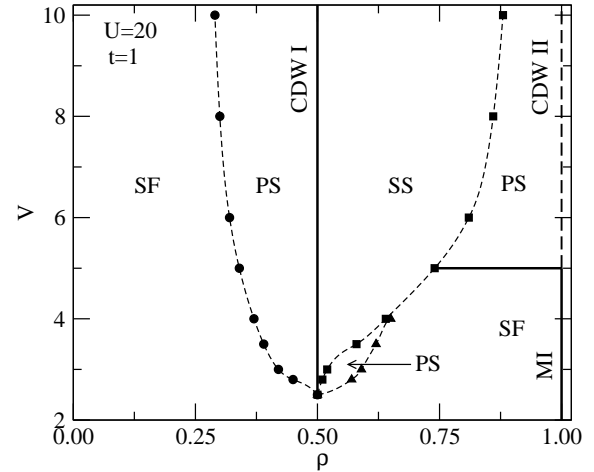


FIG. 1: The ground state phase diagram of the 2D extended Bose-Hubbard model (1) in the $V - \rho$ plane for $U/t = 20$ and densities $\rho \leq 1$, showing superfluid (SF) phases, checkerboard solids formed by single bosons (CDW I) and pairs of bosons (CDW II), a Mott-insulating phase (MI), phase separation (PS) and finally a supersolid phase (SS).

where $a_i^\dagger (a_i)$ creates (annihilates) a boson at site i with the occupation number $n_i \equiv a_i^\dagger a_i$, t is hopping, μ is the chemical potential, and $\langle i, j \rangle$ runs over all nn pairs.

In the zero-hopping limit, $t = 0$, the non-negative potential energy ($U, V > 0$) is minimized at half-filling, $\rho = 1/2$, by the crystal state with only one sublattice occupied [checkerboard pattern with (π, π) modulation in 2D]. This state is gapped; it remains stable in the presence of a small hopping, $t \ll U, V$, with a kinetic energy gain $\Delta E \approx -zt^2/[(z-1)V]$ per boson, where $z = 2d$ is the coordination number.

Introducing holes only costs chemical potential μ but no potential energy; the kinetic energy gain is somewhat increased but remains quadratic in t for isolated holes. However, the kinetic energy gain becomes *linear* in t if a number of holes encircle a region of a crystal [Fig. 2(a)]. The energy gain is maximized at $\Delta E \approx -ct$, $1 < c < 2$ per hole for a planar [linear in 2D, see Fig. 2(b)] domain wall doped with one hole per two sites. As a result, for a large system with $N = L^d$ sites, the crystalline order is

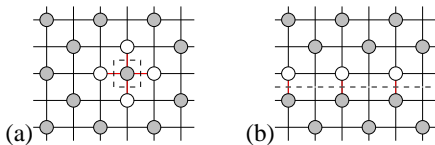


FIG. 2: The $\rho = 1/2$ checkerboard crystal doped with holes. (a) Four holes encircle a boson which can hop between the five degenerate sites. (b) Domain wall doped with holes; bosons can hop freely across the dashed line.

destroyed by introduction of a small density $\rho \sim L^{-1}$ of holes. This instability of the $\rho = 1/2$ crystal to domain wall formation upon hole doping excludes the possibility of a SS phase. In practice, on the isotropic square lattice, the instability develops further, leading to a phase separation between the commensurate crystal at $\rho = 1/2$ and a uniform superfluid with $\rho < 1/2$ (Fig. 1).

Doping of the $\rho = 1/2$ crystal with additional bosons works differently depending on the relation between V and U . The energy cost to place a boson at an empty (occupied) site is $E_0 \equiv zV - \mu$ ($E_1 \equiv U - \mu$). Respectively, for $U > zV$, the additional bosons fill empty sites and mask the checkerboard modulation; for $U - zV \gg t > 0$ the situation is precisely particle-hole conjugate to hole doping. The kinetic energy is again minimized at planar domain walls which destabilize the checkerboard crystal order. In particular, in the hard-core limit $U \rightarrow \infty$, the crystalline order is always unstable for $\rho \neq 1/2$.

With $zV \gtrsim U$, however, the bosons (unlike holes) can be placed on either an occupied or unoccupied site. The total energy of a single boson delocalized between the two sublattices is $E = E_1 + \Delta - (2z^2t^2 + \Delta^2)^{1/2}$, where $\Delta \equiv (zV - U)/2$. Clearly, for sufficiently small $\Delta \sim t$, the kinetic energy $E - E_1$ is again linear in t and large, which prevents the domain wall formation. As a result, these doped particles will form a superfluid on top of the charge ordered background and hence a supersolid. Two bosons experience both on-site and nn repulsion ($2U$ and V respectively). Therefore, at sufficiently small densities the condensate should remain stable, which completes the formal argument for the supersolid existence.

Similarly, at unit filling, $\rho = 1$, the ground state is a Mott insulator with one boson per site for $U > zV$, and an ordered solid with two bosons on every other site for $U < zV$. In the former case, additional holes (particles) move along the uniform background with the hopping integral t ($2t$) and experience both nn and on-site repulsion (infinite in the case of holes). They condense on top of the uniform background forming a superfluid. However, for $zV > U$, the doped particles move on a checkerboard background with the effective hopping, e.g., $t_* = 2t^2/[zV - U + (z - 2)V]$ for holes. The resulting kinetic energy gain is only quadratic in t and can be superseded if the holes come together into a supersolid phase with $\rho \gtrsim 1/2$. Overall, this leads to a thermodynamical instability of the hole-doped checkerboard solid formed by pairs of bosons at $\rho = 1$: the system can minimize its

energy by phase separation. Note that here phase separation is not between a superfluid and a solid but between a supersolid and a solid. The solid order is not destabilized at this first order phase transition, but just the “Bose-Einstein condensation” transition of holes doped into the solid becomes first order.

We next perform quantum Monte Carlo simulations to corroborate these arguments and to show the phase diagram and the existence of a supersolid phase for the EBHM in the low-density region $\rho \leq 1$.

We have used loop-operator updates in a stochastic series expansion (SSE) quantum Monte Carlo (QMC) method [12] to study the EBHM (1) in the strong coupling regime ($U, V \gg t$) and for $0 < \rho \leq 1$. In the present study, simulations have been carried out in square geometry, $N = L \times L$, with $L = 6, \dots, 16$. Ground state properties have been obtained by taking sufficiently large values of the inverse temperature β , where $\beta = 2L$ turned out to be sufficient.

To characterize different phases, we have studied the static staggered $[\mathbf{Q} = (\pi, \pi)]$ structure factor,

$$S(\mathbf{Q}) = \frac{1}{N} \sum_{j,k} e^{-i\mathbf{Q} \cdot (\mathbf{r}_j - \mathbf{r}_k)} \langle n_j n_k \rangle - \langle n_j \rangle^2, \quad (2)$$

which measures the diagonal long range order (checkerboard solid) in the system, and the superfluid density ρ_s , measured from the winding numbers of the bosonic world lines (W_x and W_y) in the x - and y - directions as $\rho_s = \langle W_x^2 + W_y^2 \rangle / 2\beta m$, where $m = 2/t$ is the effective mass of the bosons. A checkerboard solid ground state at $\rho = 0.5$ is marked by a diverging $S(\pi, \pi)$ and vanishing ρ_s , whereas a pure superfluid phase has $S(\pi, \pi) = 0$ and $\rho_s > 0$. A supersolid phase, on the other hand, is characterized by a diverging $S(\pi, \pi)$ and a non-zero value of ρ_s . For finite system sizes, both quantities are always finite and estimates for the thermodynamic limit are obtained by carefully studying the finite-size scaling of the observables.

A jump in ρ with varying μ indicates a discontinuous (first order) transition, and has been used to identify regions of phase separation in the canonical ensemble (fixed density ρ). We postpone a more rigorous analysis to accurately identify the nature of the transitions and the accurate domain boundaries to a later study, and focus, instead, on establishing the existence of SS phase over finite regions of the parameter space.

A plot of ρ as a function of μ shows clear indications of phase separation at $\rho < 0.5$ for all values of V —the discontinuity in ρ grows with increasing V . For $\rho > 0.5$, the curves are qualitatively different. For $V < U/4$, there is a small, but finite, region of positive slope (e.g., $0.5 < \rho < 0.52$ for $V = 3$), followed by phase separation for $0.52 < \rho < 0.60$, and a region of positive slope for $\rho > 0.6$. At $V = U/4$, there is no evidence of phase separation for $\rho > 0.5$. With $V > U/4$, the region of phase separation

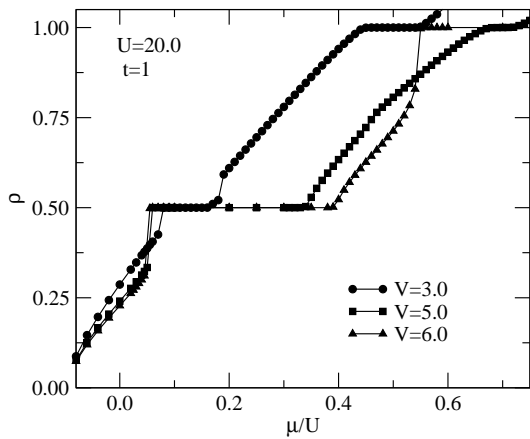


FIG. 3: The average density as a function of the chemical potential for three different values of V ($U = 20$). For clarity of presentation, data for only one system size, $L = 16$, is shown. Error bars are smaller than the symbol sizes. Discontinuous transitions are marked by finite jumps in the particle density.

shifts to large densities, $\rho \lesssim 1$. The location and extent of phase separated regions for small $V (< U/4)$ agrees well with the results of Ref. 11b apart from the extra region of positive slope for $0.5 < \rho < 0.52$. As shown below, the ground state at these densities has supersolid order. The extent of the supersolid phase decreases rapidly with decreasing V , becoming vanishingly small in the limit $V \ll U$. We note that for small V the excess density $\rho - 1/2 < 1/L$ and larger L are required to map the SS phase boundary accurately.

Ground state results for $S(\pi, \pi)$ and ρ_s as a function of ρ for three representative values of V are shown in Fig. 4 for three different system sizes L . The data are seen to be well converged with system size. At small ρ , the ground state is a superfluid (SF)—the stiffness converges to a finite value while $S(\pi, \pi)$ scales to zero. As the density increases beyond a critical value n_{c1} , there is a discontinuous transition to a (π, π) ordered charge-density-wave (CDW) ground state with $\rho = 0.5$. Any intermediate density is inaccessible in the grand canonical ensemble. For $V = 3t (< U/4)$, at $\rho > 0.5$, there are indications for a small region of supersolid (SS) characterized by finite values of *both* $S(\pi, \pi)$ and ρ_s , but further finite size scaling tests will be needed to check whether this region remains in the thermodynamic limit. With increasing density, there is another discontinuous transition to an SF state with a second region of PS. Finally, at $\rho = 1$, the ground state is a Mott insulator (MI) with both $S(\pi, \pi) = 0$ and $\rho_s = 0$. For $V = 5t (= U/4)$, the extent of the SS region increases substantially and its stability is well established. Additionally, the second phase separated region shrinks to zero and there is a direct SS-SF transition. For $V = 6t (> U/4)$, the SF phase at high densities is replaced by another region of phase separation. The ground state at $\rho = 1$ changes from a MI to a (π, π) ordered CDW state with two particles occupying every alternate lattice site, with a discontinuous

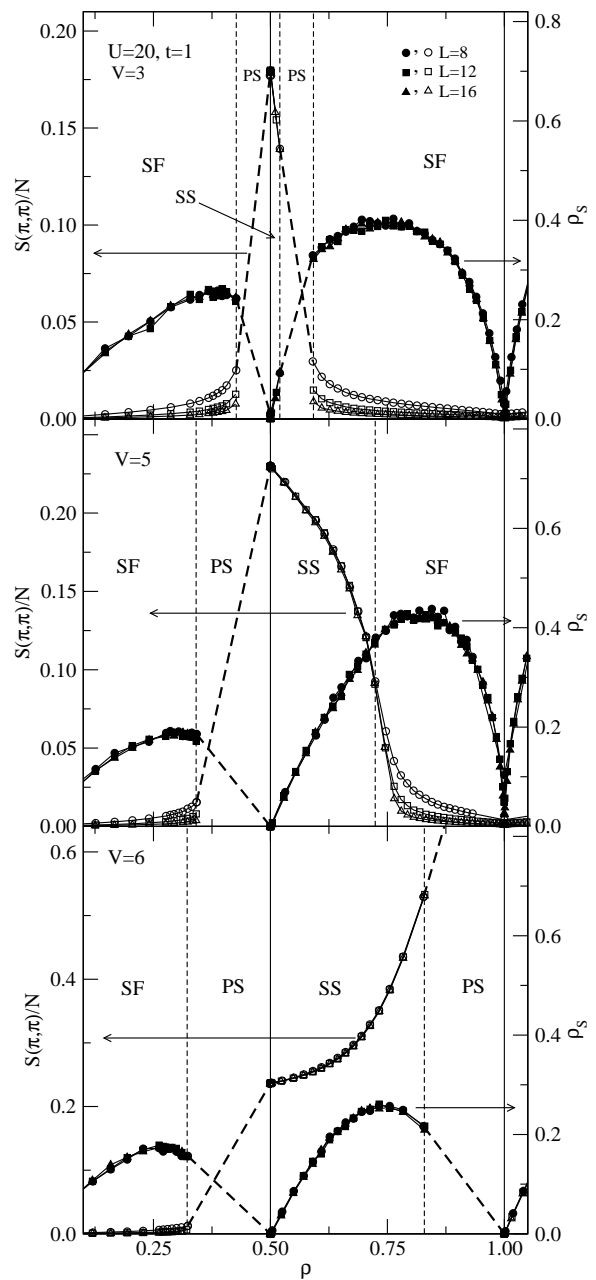


FIG. 4: The scaled static staggered structure factor (open symbols) and superfluid stiffness (filled symbols) as a function of average particle density ρ for three representative values of V . At small ρ , the ground state is a superfluid (SF) for all V . With increasing density there is discontinuous transition to a (π, π) -ordered charge density wave (CDW) at $\rho = 0.5$, with an intermediate region of phase separation (PS). At $\rho \gtrsim 0.5$, the ground state is a supersolid (SS) with finite values of both $S(\pi, \pi)$ and ρ_s . For $V < U/4$, this is followed by another discontinuous transition to a SF (the precise mapping of the SS/PS boundary requires larger L), with a second region of PS. For $V = U/4$, the SS region extends to higher densities with a continuous transition to a SF ground state at $\rho \approx 0.74$. The SS state extends to even higher densities for $V > U/4$, but is followed by a discontinuous transition to a (π, π) -ordered CDW at $\rho = 1$, with an accompanying region of PS. For $V \leq U/4$, the ground state at $\rho = 1$ is a Mott insulator.

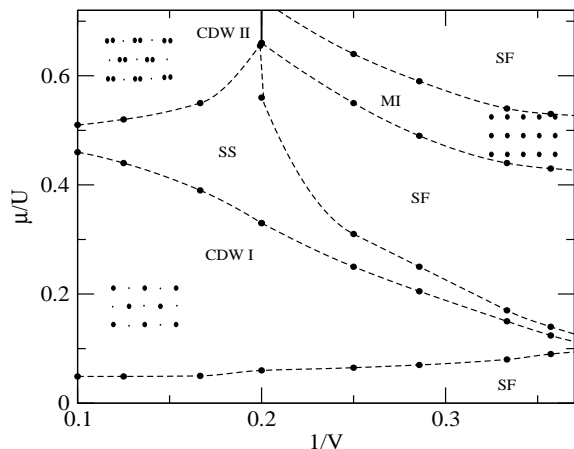


FIG. 5: The ground state phase diagram in the $V - \mu$ plane, notations as in Fig. 1. Different solid-ordered phases are shown schematically. The PS regions are manifested as discontinuous transitions across the corresponding phase boundaries (not shown).

transition separating it from the SF state.

The results are combined to map the schematic ground state phase diagram of the Hamiltonian (1) in the $V - \rho$ (Fig. 1) and $\mu - 1/V$ (Fig. 5) planes. Fig. 1 shows the different phases in the (V, ρ) parameter space at a constant value of the on-site interaction, $U = 20$, $t = 1$. For small V , the ground state is a SF for all $\rho < 1$. At $V > 2.5t$, the different phases appear as shown in the figure. The extent of the supersolid phase and that of the phase separated region at $\rho < 0.5$ increases with increasing V , whereas the phase separated region at $\rho > 0.5$ gets vanishingly small for moderate values of V . It is not clear from the available data if the PS-SF phase boundary meets the SS boundary at a point, or approaches it asymptotically. At $V > 5.0t$, the SF region at high densities is replaced by a phase separated region, while the ground state at $\rho = 1$ changes from a MI to a (π, π) -ordered CDW with two bosons occupying every other lattice site. It should be emphasized that the phase diagram is qualitative and the phase boundaries are approximate.

The features of the phase diagram as a function of $1/V$ (Fig. 5) are markedly different from the “lobe” structure observed in a plot of μ as a function of t/U for the EBHM. The nature of the ground state at $\rho = 1$ changes from a CDW to an MI as V is varied across $U/4$. This is accompanied by a change in the curvatures of the phase boundaries. Furthermore, the MI region remains finite even in the limit of $V \rightarrow 0$. No evidence of supersolid phase is found at $\rho = 0.5$, in agreement with the variational studies and previous numerics [7, 9].

In conclusion, we have used exact strong-coupling expansion and QMC simulations to study the nature of the ground state phases of the extended boson-Hubbard model on a square lattice. The interplay of the on-site and nearest-neighbor interactions leads to a rich phase

diagram including a supersolid phase with simultaneous diagonal and off-diagonal long-range order. We have provided strict arguments why a soft-core model with $V > U/z$ and densities $\rho > 1/2$ is sufficient to stabilize a supersolid phase in a model with nearest neighbor couplings only. This is in contrast to the “hard-core” bosons where the system phase separates for all values of the nn interaction strength and additional nnn interactions or hoppings are needed to stabilize a supersolid ground state. Also, in the studied range of parameters (including very large $V < 12t$) we have not found any nominally gapless phase with both $S(\pi, \pi)$ and ρ_s zero which could potentially be identified with a bose metal [13] (see also the argument against such a phase in Ref. 11d).

It is a pleasure to thank N. Prokof'ev, B. Svistunov, and C. M. Varma for useful discussions and R. T. Scalettar for suggesting the problem. Simulations were carried out on the computer cluster at the Institute of Geophysics and Planetary Physics at the University of California, Riverside.

-
- [1] E. Kim and M. H. W. Chan, *Nature* **427**, 225 (2004); *Science* **305**, 1941 (2004).
 - [2] A. Leggett, *Science* **305**, 1921 (2004); N. Prokof'ev, and B. Svistunov, preprint cond-mat/0409472; A. S. Moskovin, I. G. Bostrem, and A. S. Ovchinnikov, preprint cond-mat/0404561.
 - [3] O. Penrose, and L. Onsager, *Phys. Rev.* **104**, 576 (1956).
 - [4] A. F. Andreev, and I. M. Lifshitz, *Sov. Phys. JETP* **29**, 1107 (1960); G. Chester, *Phys. Rev. A* **2**, 256 (1970); A. J. Leggett, *Phys. Rev. Lett.* **25**, 1543 (1970).
 - [5] P. W. Anderson, *Basic notions of Condensed Matter Physics* (Benjamin, New York, 1984).
 - [6] For review of experimental and theoretical work see M. W. Meisel, *Physica* **178B**, 121 (1992), and other articles in the same volume.
 - [7] H. Matsuda, and T. Tsuneto, *Suppl. Prog. Theor. Phys.* **46**, 411 (1970); K. S. Liu, and M. E. Fisher, *J. Low Temp. Phys.* **10**, 655 (1973); E. Roddick and D. Stroud, *Phys. Rev. B* **48**, 16600 (1993); *ibid.* **51**, 8672 (1995). G. G. Batrouni *et al.*, *Phys. Rev. Lett.* **74**, 2527 (1995); R. T. Scalettar *et al.*, *Phys. Rev. B* **51**, 8467 (1995); R. Mincas, S. Robaszkiewicz, and T. Kostyrko, *ibid.* **52**, 6863 (1995); E. S. Sorensen and E. Roddick, *ibid.* **53**, R8867 (1996).
 - [8] E. Frey and L. Balents, *Phys. Rev. B* **55**, 1050 (1997).
 - [9] A. van Otterlo and K.-H. Wagenblast, *Phys. Rev. Lett.* **72**, 3598 (1994); A. van Otterlo *et al.*, *Phys. Rev. B* **52**, 16176 (1995).
 - [10] M. Greiner *et al.*, *Nature* **415**, 39 (2002).
 - [11] Kohno and Takahashi, *Phys. Rev. B* **56**, 3212 (1997); G. G. Batrouni, and R. T. Scalettar, *Phys. Rev. Lett.* **84**, 1599 (2000); H. Hébert *et al.*, *Phys. Rev. B* **65**, 014513 (2001); A. Kuklov, N. Prokof'ev, and B. Svistunov, *Phys. Rev. Lett.* **93**, 230402 (2004).
 - [12] A. W. Sandvik, *Phys. Rev. B* **59**, R14157 (1999).
 - [13] P. Phillips, and D. Dalidovich, *Science* **302**, 243 (2003); S. Das, and S. Doniach, *Phys. Rev. B* **64**, 134511 (2001); *ibid.* **60**, 1261 (1998).